European Journal of Radiology Open 8 (2021) 100352

Contents lists available at ScienceDirect

European Journal of Radiology Open

journal homepage: www.elsevier.com/locate/ejro

# Intravenous enhanced 3D FLAIR imaging to identify CSF leaks in spontaneous intracranial hypotension: Comparison with MR myelography

Iichiro Osawa [a,*], Eito Kozawa [a], Takashi Mitsufuji [b], Toshimasa Yamamoto [b], Nobuo Araki [b], Kaiji Inoue [a], Mamoru Niitsu [a]

[a] Department of Radiology, Saitama Medical University Hospital, 38 Morohongo, Moroyama-machi, Iruma-gun, Saitama, 350-0495, Japan
[b] Department of Neurology, Saitama Medical University Hospital, 38 Morohongo, Moroyama-machi, Iruma-gun, Saitama, 350-0495, Japan

ARTICLE INFO

*Keywords:*
Spinal cerebrospinal fluid leak
Spontaneous intracranial hypotension
Heavily T2-weighted 3D FLAIR
Intravenous gadolinium-enhanced MR imaging
MR myelography

ABSTRACT

*Purpose:* To evaluate the clinical utility of intravenous gadolinium-enhanced heavily T2-weighted 3D fluid-attenuated inversion recovery (HT2-FLAIR) imaging for identifying spinal cerebrospinal fluid (CSF) leaks in patients with spontaneous intracranial hypotension (SIH).

*Methods:* Patients with SIH underwent MR myelography and post-contrast HT2-FLAIR imaging after an intravenous gadolinium injection. Two types of CSF leaks (epidural fluid collection and CSF leaks around the nerve root sleeve) at each vertebral level were compared between the 2 sequences. The total numbers of CSF leaks and vertebral levels involved were recorded for the whole spine. The sequence that was superior for the overall visualization of epidural and paraspinal fluid collection was then selected.

*Results:* Nine patients with SIH were included in the present study. HT2-FLAIR imaging was equivalent or superior to MR myelography at each level for detecting the 2 types of CSF leaks. In the 2 types of CSF leaks, the total numbers of CSF leaks and levels involved were higher on HT2-FLAIR images than on MR myelography, while no significant difference was observed for CSF leaks around the nerve root sleeve. In all 9 patients, HT2-FLAIR imaging was superior to MR myelography for the overall visualization of epidural and paraspinal fluid collection.

*Conclusion:* Intravenous gadolinium-enhanced HT2-FLAIR imaging was superior to MR myelography for the visualization of CSF leaks in patients with SIH. This method can be useful for identifying spinal CSF leaks.

## 1. Introduction

Spontaneous intracranial hypotension (SIH) is caused by spontaneous cerebrospinal fluid (CSF) leaks from the spine. Although the mechanisms underlying spontaneous CSF leaks remain unclear, a combination of weak spinal meninges and trauma is generally suspected. Previous studies reported relationships between CSF leaks and various factors related to meningeal weakness, including meningeal diverticula, bony osteophytes, and calcified intervertebral discs [1]. Since SIH shows a broad spectrum of clinical and imaging manifestations [2], the diagnosis of this condition remains challenging and, thus, it is often misdiagnosed [3]. Clinical manifestations are generally characterized by orthostatic headache and low CSF pressure. However, different types of headaches as well as focal or generalized neurological abnormalities have been reported, and normal CSF pressure is not uncommon in patients with SIH [4].

Imaging manifestations of the brain and spine are typically explained by spinal CSF leaks, followed by CSF volume losses and subsequent compensatory responses (the Monro-Kellie doctrine). One of the characteristic features on brain magnetic resonance imaging (MRI) is diffuse pachymeningeal enhancement; however, this is not observed in approximately 20 % of patients with SIH [5]. In contrast, spinal imaging,

*Abbreviations:* CHESS, Chemical shift selective; CSF, Cerebrospinal fluid; FLAIR, Fluid-attenuated inversion recovery; HT2-FLAIR, Heavily T2-weighted fluid-attenuated inversion recovery; MIP, Maximum intensity projection; MPR, Multiplanar reconstruction; MRI, Magnetic resonance imaging; SIH, Spontaneous intracranial hypotension; T1W, T1-weighted; T2W, T2-weighted; TSE, Turbo spin echo.

* Corresponding author at: 38 Morohongo, Moroyama-machi, Iruma-gun, Saitama, 350-0495, Japan.
*E-mail addresses:* oyabun@saitama-med.ac.jp (I. Osawa), 8kozawa@saitama-med.ac.jp (E. Kozawa), mitsufuj@saitama-med.ac.jp (T. Mitsufuji), ytoshi@saitama-med.ac.jp (T. Yamamoto), arakin@saitama-med.ac.jp (N. Araki), kaiji@saitama-med.ac.jp (K. Inoue), niitsu@saitama-med.ac.jp (M. Niitsu).

https://doi.org/10.1016/j.ejro.2021.100352
Received 27 March 2021; Received in revised form 27 April 2021; Accepted 8 May 2021

including CT myelography [6], digital subtraction myelography [7], MRI [8], MR myelography [9,10], intrathecal gadolinium-enhanced MR myelography [6,11], and radioisotope cisternography [12], mainly allows for the detection of CSF leaks [1]. CT myelography is a reliable technique for identifying the exact sites of CSF leaks, with good spatial resolution and the rapid acquisition of images [6]. Despite its clinical advantages, radiation exposure is a cause of concern for patients who undergo this examination. Intrathecal gadolinium-enhanced MR myelography typically creates images based on fat-suppressed T1-weighted (T1W) imaging with a diluted contrast agent [11,13]. This technique has no risk of radiation exposure, while the intrathecal injection of a gadolinium-based contrast agent is off-label use in Japan and worldwide. Radioisotope cisternography allows for long-term observations of CSF leaks [12]. However, this technique does not show the precise localization of a leak because of poor spatial resolution and inferior anatomical delineations. Furthermore, since this method may not be used to accurately discriminate CSF leaks within the epidural space from CSF within the subarachnoid space, its sensitivity for detecting a small epidural CSF leak may be low. The greatest disadvantages of these 3 techniques are their invasiveness and the complexity of the procedure, which is mainly attributed to lumbar puncture. Other drawbacks include iatrogenic CSF leaks [14] and worsening symptoms [15] caused by lumbar puncture. Therefore, non-contrast spinal MRI may be used as the first-line method of choice for the diagnosis of CSF leaks, including fat-suppressed T2-weighted (T2W) imaging and MR myelography.

MR myelography is based on heavily T2W sequences and enhances CSF signals by suppressing the adjacent background signal. This method has been increasingly applied in clinical practice using 2D [9,16,17] or 3D [10,18] sequences. Previous studies reported similarities between MR myelography and CT myelography [17] or radioisotope scintigraphy [16]. Nevertheless, non-contrast MR imaging has the following limitations: the unclear definition of CSF leaks [10], difficulty differentiating between CSF leaks and tissues with similar signal intensities [8,19], and the requirement for homogenous fat suppression [1].

Fluid-attenuated inversion recovery (FLAIR) is an MRI sequence with inversion recovery to suppress signals from water. FLAIR imaging provides greater sensitivity for detecting subtle T1-shortening induced by contrast material than T1W imaging, and has been applied to various intracranial lesions [20]. However, to the best of our knowledge, the enhancement of spinal CSF leaks in patients with SIH has not been observed using intravenous gadolinium-enhanced T1W imaging or FLAIR imaging. Heavily T2W 3D FLAIR (HT2-FLAIR) is a variant of the 3D turbo spin echo (TSE) FLAIR sequence with variable flip-angle refocusing pulses [21]. This sequence allows for greater sensitivity to low concentrations of contrast material than conventional 3D FLAIR, and has been applied to the inner ear and brain [20]. A previous study demonstrated that the anterior eye segment and various areas of the cranial subarachnoid space were enhanced on HT2-FLAIR in patients without eye disease or subarachnoid space disease [22]. In our clinical practice, we noted that CSF leaks at the posterior upper neck were enhanced when patients with SIH underwent gadolinium-enhanced HT2-FLAIR imaging for head evaluations. The purpose of the present study was to assess the clinical utility of intravenous gadolinium-enhanced HT2-FLAIR imaging by comparing the visualization of CSF leaks to MR myelography at 3 T.

## 2. Materials and methods

### 2.1. Patients

This retrospective study was conducted at a single institution and approved by the Institutional Review Board of our institution. We obtained written informed consent for the procedures and opt-out consent for the use of retrospective clinical data from all patients/ from parents or legal guardian of patient less than 18 years. We reviewed the imaging records of 12 consecutive patients diagnosed with SIH according to the criteria proposed by Shievink [23] or the Headache Classification Committee of the International Headache Society, 3rd edition (ICHD-3) [24] between November 2018 and July 2020. Patients who met the following inclusion criteria were enrolled: 1) spinal MR myelography was available, 2) spinal HT2-FLAIR imaging with and without gadolinium-based contrast material was available, and 3) CSF leaks were identified by spinal MR myelography. Patients were excluded if image quality was insufficient for image interpretation.

### 2.2. MRI

All MRI examinations were performed using the 3 T MRI unit (MAGNETOM Skyra, Siemens, Erlangen, Germany) with a phased-array spinal coil. All patients with SIH underwent MRI of the whole spine, which was scanned using 2 separate FOVs (the cervicothoracic and thoracolumbosacral spines) with partial overlapping at the edges of the scans.

All examinations consisted of the following 3 images: sagittal MR myelography and pre- and post-contrast sagittal HT2-FLAIR images. The parameters of MRI are summarized in Table 1. Post-contrast sagittal HT2-FLAIR images were obtained immediately after an intravenous injection of gadolinium-HP-DO3A (Gadoteridol) at a single dose of 0.2 mL/kg (0.1 mmol/kg).

We reconstructed axial and coronal multiplanar reconstruction (MPR) images with thin slices from sagittal MR myelography and HT2-FLAIR imaging. Subtraction images were generated by subtracting initial pre-contrast HT2-FLAIR images from the corresponding post-contrast HT2-FLAIR images. Cases 4 and 5 in Table 2 underwent sagittal fat-suppressed T2W imaging at the thoracolumbosacral level. Additionally, in case 4, pre-contrast MR cisternography, HT2-FLAIR, and fat-suppressed T1W spin echo imaging of the head were performed followed by post-contrast HT2-FLAIR and fat-suppressed T1W spin echo imaging after post-contrast spinal HT2-FLAIR imaging.

### 2.3. Imaging analysis

MR myelography and HT2-FLAIR images were evaluated independently in a random order by 2 board-certified radiologists with 10 and 30 years of experience, respectively. The readers reviewed these images in 3 orthogonal planes (sagittal, reformatted axial, and reformatted coronal), and were blinded to clinical information and sequence parameters. Any discrepancies between the readers were resolved through discussion until a consensus was reached.

The MRI review was performed in 2 sessions. In the first session, readers were asked to count CSF leaks, including epidural and paraspinal fluid collection, at each vertebral level. Epidural fluid collection

**Table 1**
Scan parameters of spinal MRI.

| | MR myelography | HT2-FLAIR |
|---|---|---|
| TR/TE (ms) | 4000/425 | 9000/541 |
| Inversion time (ms) | – | 2250 |
| CHESS fat suppression prepulse | + | + |
| Flip angle | Average flip angle 110° | Average flip angle 110° |
| Echo train length | 519 | 519 |
| Matrix size | 384 × 384 | 384 × 384 |
| FOV ($mm^2$) | 350 × 350 | 350 × 350 |
| Sagittal slices | 128 | 128 |
| In-plane resolution (mm) | 0.9 × 0.9 | 0.5 × 0.5 (after interpolation) |
| Slice thickness (mm) | 0.9 | 0.9 |
| Bandwidth (Hz/pixel) | 434 | 434 |
| Acceleration factor | 2 using GRAPPA | 3 using GRAPPA |
| Number of excitations | 1.4 | 1.4 |
| Total time (min) | 3.42 | 5.26 |

*CHESS* chemical shift selective.

**Table 2**
Clinical characteristics and spinal MRI of patients with SIH (n = 9).

| Patient No. | Age (years) | Sex | Symptoms | CSF pressure ($cmH_2O$) | Spinal MRI findings | | |
|---|---|---|---|---|---|---|---|
| | | | | | Epidural fluid collection (location) | Paraspinal fluid collection (location) | C1−2 sign |
| 1 | 14 | F | Headache | NA | + (S) | – | – |
| 2 | 60 | F | Orthostatic headache | 9.2 | + (S) | – | – |
| 3 | 32 | F | Orthostatic headache, tinnitus | NA | + (T/S) | – | – |
| 4 | 50 | F | Orthostatic headache, tinnitus, ear fullness | NA | + (C/T/L/S) | + (C/L) | + |
| 5 | 16 | M | Headache | NA | + (S) | – | – |
| 6 | 40 | F | Headache, tinnitus, sensorineural hearing loss | NA | + (T) | + (C/T) | – |
| 7 | 52 | F | Headache, sensorineural hearing loss | NA | + (T) | + (T) | – |
| 8 | 28 | M | Headache, nausea | NA | + (C/T/L/S) | + (C/T/L) | + |
| 9 | 31 | M | Orthostatic headache, nausea | NA | + (C/T/L/S) | + (C/T/L) | + |

*NA* not available, *C* cervical spine, *T* thoracic spine, *L* lumbar spine, *S* sacral spine.

represents the fluid signal intensity outside the dura mater within the spinal canal [8,9,17,25], and was divided into 3 types based on its location relative to the dural sac: 1) fluid mainly located ventral to the dural sac, 2) fluid circularly surrounding the dural sac, and 3) fluid mainly located dorsal to the dural sac [25]. The ventral or dorsal leak was counted as 1 leak at each level (C1 to L5), while the circular leak was counted as 2 leaks. Paraspinal fluid collection is defined as the fluid signal around the outside of the spine, including CSF leaks around the nerve root sleeve and the C1−2 sign [8,9,17]. The C1−2 sign is referred to as fluid signal intensity in soft tissues at C1−2 [26]. A right or left leak around the nerve root sleeve was counted as 1 leak at each level (C1−2 to L2−3), while bilateral leaks were counted as 2 leaks. Other paraspinal CSF leaks, such as the C1−2 sign, were not included in the CSF leak count. Furthermore, the total numbers of CSF leaks and vertebral levels involved were recorded at the whole spine.

In the second reading session, each reader individually compared both sequences side-by-side, and was asked of their overall preferred sequence for the visualization of CSF leaks, including epidural and paraspinal fluid collection. We herein evaluated all cases of epidural (including CSF leaks at the S level) and paraspinal fluid collection (including CSF leaks in the interspinous space and the C1−2 sign).

### 2.4. Statistical analysis

The Wilcoxon signed-rank test was used to evaluate whether the sequence affected the detection of the total numbers of CSF leaks and vertebral levels involved or the visualization of CSF leaks. Values represented the mean per patient ± standard deviation. JMP 14.0.0 software (SAS Institute, Cary, NC, USA) was used for statistical analyses. Two-tailed $p$ values less than 0.05 were considered to be significant.

## 3. Results

### 3.1. Patients

We identified 12 patients with SIH. Nine patients underwent MR myelography and HT2-FLAIR imaging with and without gadolinium-based contrast material. Of the 9 patients with available spinal images, all showed CSF leaks identified by MR myelography. Furthermore, among the 9 patients who satisfied the inclusion criteria, none met the exclusion criteria. Patient characteristics are summarized in Table 2. The patient cohort included 3 males and 6 females, with an average age of 36 years (range, 14–60 years).

### 3.2. Comparison between MR myelography and HT2-FLAIR imaging

Fig. 1 shows that HT2-FLAIR imaging was equivalent or superior to MR myelography at each level for detecting the 2 types of CSF leaks (epidural fluid collection and CSF leaks around the nerve root sleeve). Regarding epidural fluid collection, the total numbers of CSF leaks and levels involved were higher on HT2-FLAIR images than on MR myelography (CSF leaks; 31.9 ± 29.9 vs 10.7 ± 10.9, $p = 0.031$, levels involved; 12.2 ± 10.9 vs 8.4 ± 8.3, $p =$ 0.031). Regarding CSF leaks around the nerve root sleeve, the total numbers of CSF leaks and levels

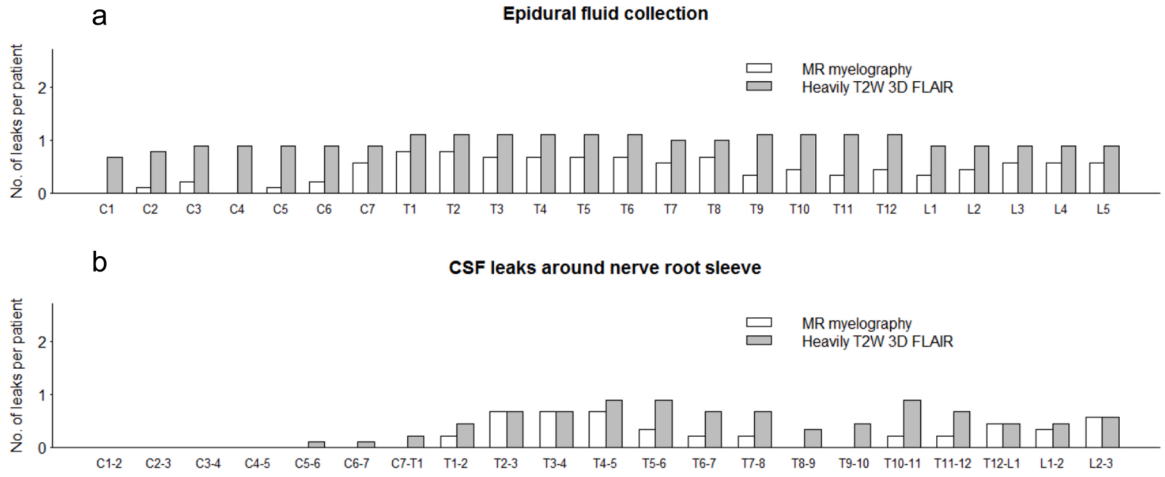


**Fig. 1.** Distribution of CSF leaks on MR myelography and HT2-FLAIR images. Two types of CSF leaks are most commonly observed at the T level (epidural fluid collection in (a) and CSF leaks around the nerve root sleeve in (b)).

involved were slightly higher on HT2-FLAIR images than on MR myelography (CSF leaks; 9.1 ± 10.5 vs 4.8 ± 6.6, $p = 0.13$, levels involved; 4.9 ± 5.6 vs 2.8 ± 3.6, $p = 0.13$).

HT2-FLAIR imaging was superior to MR myelography in all 9 patients for the overall visualization of epidural fluid collection ($p = 0.004$) and paraspinal fluid collection ($p = 0.004$) (Figs. 2–5). There was no contrast enhancement in the meningeal diverticula (Fig. 6), dilated epidural venous plexus (Fig. 7), or subarachnoid space (Figs. 2–5,7, and 8).

In cases 4 and 5, CSF leaks were more strongly enhanced than the epidural venous plexus and/or basivertebral vein on post-contrast HT2-FLAIR images (Figs. 4 and 5). Regarding post-contrast HT2-FLAIR imaging of the head in case 4, the C1−2 sign and epidural fluid collection showed contrast enhancement, while the suboccipital cavernous sinus and epidural venous plexus did not or only showed weak contrast enhancement (Fig. 8).

## 4. Discussion

The present study demonstrated the clinical utility of intravenous gadolinium-enhanced HT2-FLAIR imaging for the visualization of spinal CSF leaks in patients with SIH. HT2-FLAIR imaging identified more CSF leaks and vertebral levels involved, and the overall visualization of CSF leaks was superior to that with MR myelography.

MR myelography is based on heavily T2W sequences and may enhance CSF signals by suppressing the adjacent background signal. This method has become increasingly available in clinical practice using 2D [9,16,17] or 3D [10,18] sequences. The major advantages of MR myelography include no radiation exposure, no need for lumber puncture or the intrathecal administration of contrast material or a radioactive isotope, and multiple imaging planes. Previous studies reported similarities between MR myelography and CT myelography [17] or radioisotope cisternography [16] for CSF leak detection. However, other fluid-filled structures (paravertebral veins and the cystic dilatation of nerve root sleeves or meningeal diverticula) or unsuppressed fat, both of which exhibit hyperintensity on MR myelography similar to that of CSF, may be misinterpreted as CSF leaks because the suppression of background signals may cause poor anatomical orientation.

2D single thick-slice MR myelography provides better background suppression from paravertebral veins or fat with shorter acquisition times than multislice MR myelography [27]. Thick-slice acquisition in a coronal or sagittal direction allows for delineation of the whole spine in a single projection image and does not require a postprocessing procedure, such as maximum intensity projection (MIP). However, a single projection image cannot be reconstructed in other directions, which makes additional image acquisitions necessary at desirable angles. Furthermore, 2D single thick-slice MR myelography may not have the capacity to differentiate between epidural CSF leaks and subarachnoid CSF, particularly on coronal images, because low spatial resolution obscures details in the dura mater between the 2 fluid-filled spaces. In the present study, we used 3D MR myelography in which a 3D data set generates MPR images of arbitrarily reformatted directions as well as MIP images for a panoramic view.

FLAIR is an MRI sequence with inversion recovery to a null signal intensity from water. This technique provides greater sensitivity for detecting subtle T1-shortening induced by contrast material than T1W imaging, and has been applied to various intracranial lesions [20]. 3D FLAIR offers higher spatial resolution and fewer CSF flow artifacts than 2D FLAIR [28]. The 3D sequence allows for the reconstruction of image data using various techniques, including MIP and MPR. This technique can also suppress the vessel signal and promote the recognition of subarachnoid pathologies [29]. HT2-FLAIR is a variant of the 3D TSE FLAIR sequence with variable flip-angle refocusing pulses [21]. This sequence allows for greater sensitivity to low concentrations of contrast material than conventional 3D FLAIR, and has been applied to the inner ear and brain [20]. Furthermore, heavily T2 weighting is used to produce images

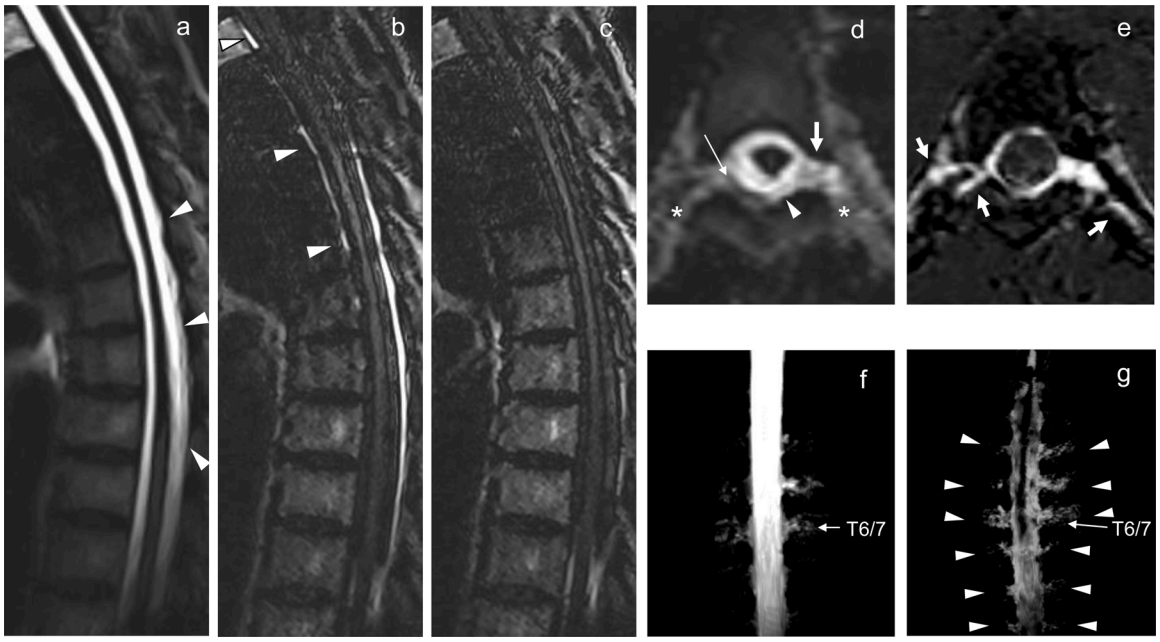


**Fig. 2.** A 52-year-old female with SIH (case 7). Sagittal MR myelography (a) shows epidural fluid collection within the spinal canal dorsal to the dural sac at T5-8 (arrowheads). Epidural fluid collection ventral to the dural sac is invisible. Sagittal post-contrast HT2-FLAIR imaging (b) reveals contrast enhancement within the spinal canal that was absent in pre-contrast imaging (c), corresponding to epidural fluid collection shown in A. Note that enhanced CSF leaks are more widely distributed at T4, T9-11 dorsal, and T1-6 ventral to the dural sac (arrowheads). Axial MR myelography (d) shows CSF leaks in the dorsal epidural space (arrowhead) and around the left T6 nerve root sleeve (arrow). Unsuppressed fat, which is slightly hyperintense, obscures the CSF leak (asterisks). The dura mater is visible as a hypointense band-like structure (small arrow). Axial subtraction HT2-FLAIR imaging (e) depicts CSF leaks circularly surrounding the dural sac and around bilateral nerve sleeves (arrows). CSF is not enhanced in the subarachnoid space. MIP of MR myelography (f) provides a panoramic view of CSF leaks, with CSF leaks around the nerve root sleeves being more conspicuous on MIP of subtracted HT2-FLAIR imaging (g, arrowheads). Of note, epidural fluid collection, which was not differentiated from subarachnoid CSF on MIP of myelography, is clearly visible.

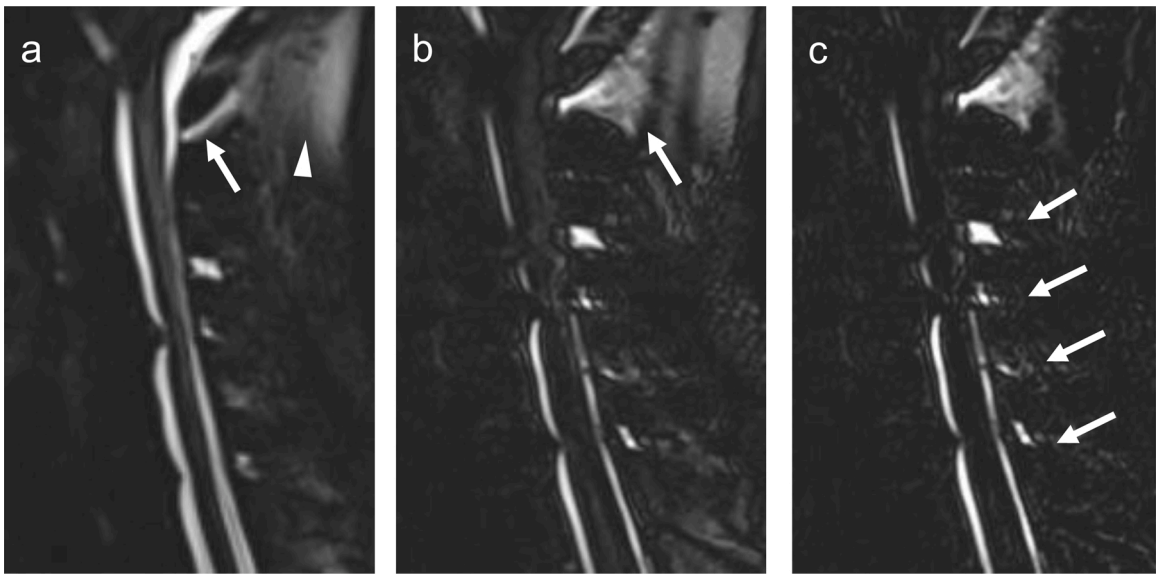


**Fig. 3.** A 50-year-old female with SIH (case 4). Sagittal MR myelography (a) shows retrospinal fluid collection at C1-2 (arrow) also known as the C1-2 sign. Unsuppressed paraspinal and subcutaneous fat is observed in the posterior neck (arrowhead), obscuring or mimicking the CSF leak. Sagittal post-contrast HT2-FLAIR imaging (b) shows the enhancement of the retrospinal CSF leak (arrow), which is more clearly visible on subtracted HT2-FLAIR images (c) due to the canceling of the fat signal. Paraspinal CSF leaks in the interspinous space are also noted at C3-4 to C6-7 (arrows).

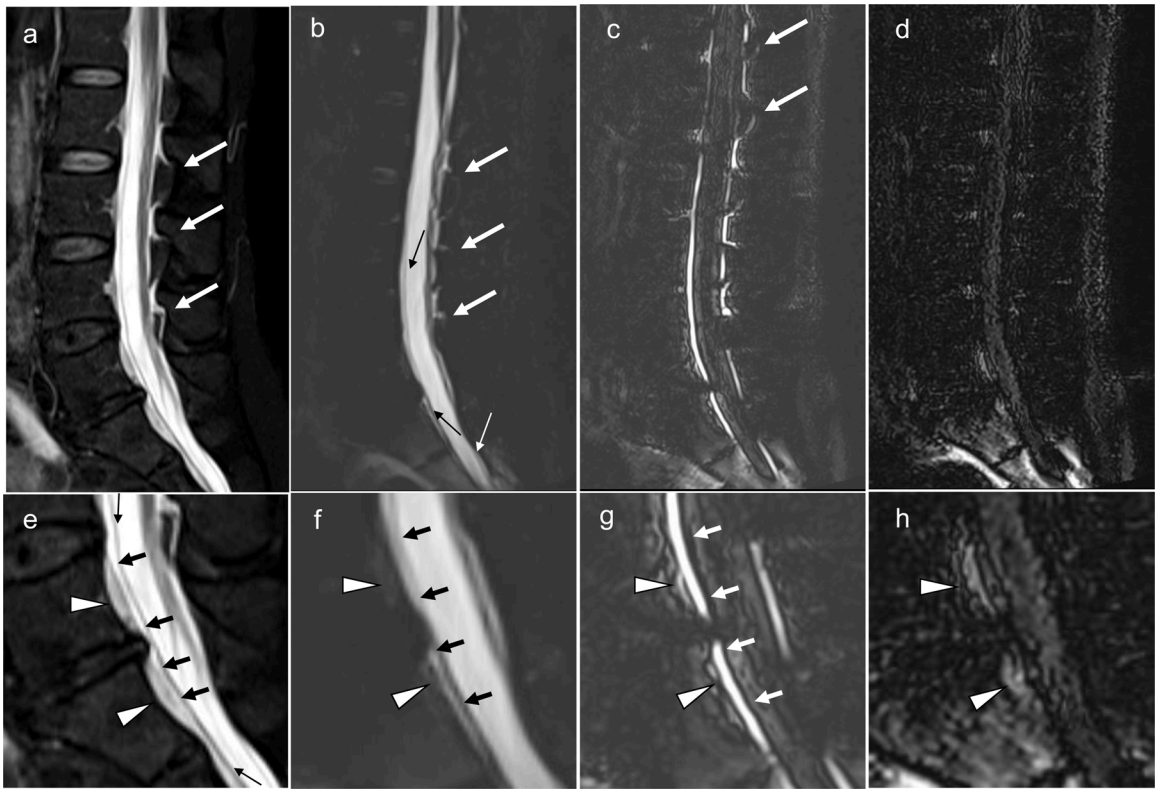


**Fig. 4.** A 50-year-old female with SIH (case 4, same patient as in Fig. 3). Sagittal fat-suppressed T2W imaging (a) displays subtle arched hyperintensities in the interspinous epidural space at the lumbar level (arrows), termed the "Dinosaur tail sign", which may reflect a subtle amount of CSF leakage. MR myelography (b) shows this sign at L2-3 to L4-5 (arrows). This sign is stronger on post-contrast HT2-FLAIR images (c) than on pre-contrast images (d), and is more conspicuous, particularly at T12-L1 and L1-2 (arrows). Epidural fluid collection, which is observed dorsal and ventral to the dural sac as a hypointense line (b, small arrows), is also more clearly visible. Each image in the lower row (e-h) shows the magnification of the lumbosacral traditional area in the upper row (a-d). On fat-suppressed T2W images (e), epidural venous plexuses (arrowheads) are more hypointense than epidural fluid collection (arrows) ventral to the dura mater (small arrows). MR myelography (f) shows that epidural venous plexuses (arrowheads) are more hypointense than epidural fluid collection (arrows), indicating stronger contrast between veins and fluid than on fat-suppressed T2W images. Of note, post-contrast HT2-FLAIR imaging (g) showed no or the weaker enhancement of veins (arrowheads) than that of CSF leaks (arrows). These venous structures are mildly hyperintense on pre-contrast HT2-FLAIR images (h, arrowheads).

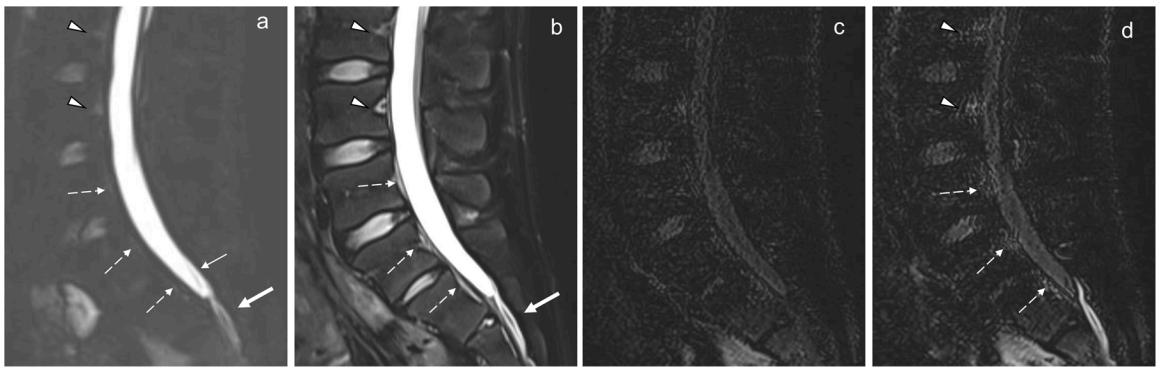


**Fig. 5.** A 16-year-old male with SIH (case 5). Sagittal MR myelography (a) and fat-suppressed T2W imaging (b) show linear-shaped fluid collection (arrow) within sacral epidural fat caudally extending from the distal termination of the dural sac, which reflects an epidural CSF leak. The filum terminale internum (a, small arrow) fuses with the distal end of the dura mater. The basivertebral veins (arrowheads) and epidural venous plexuses (dotted arrows) are mildly hyperintense on MR myelography (a), while these venous structures exhibit hyperintensity on fat-suppressed T2W imaging (b). In contrast to pre-contrast HT2-FLAIR imaging (c), post-contrast HT2-FLAIR imaging (d) shows the marked enhancement of the CSF leak and greater conspicuity than MR myelography. Of note, post-contrast HT2-FLAIR imaging shows no or only the weak enhancement of the veins described above (d, arrowheads and dotted arrows).

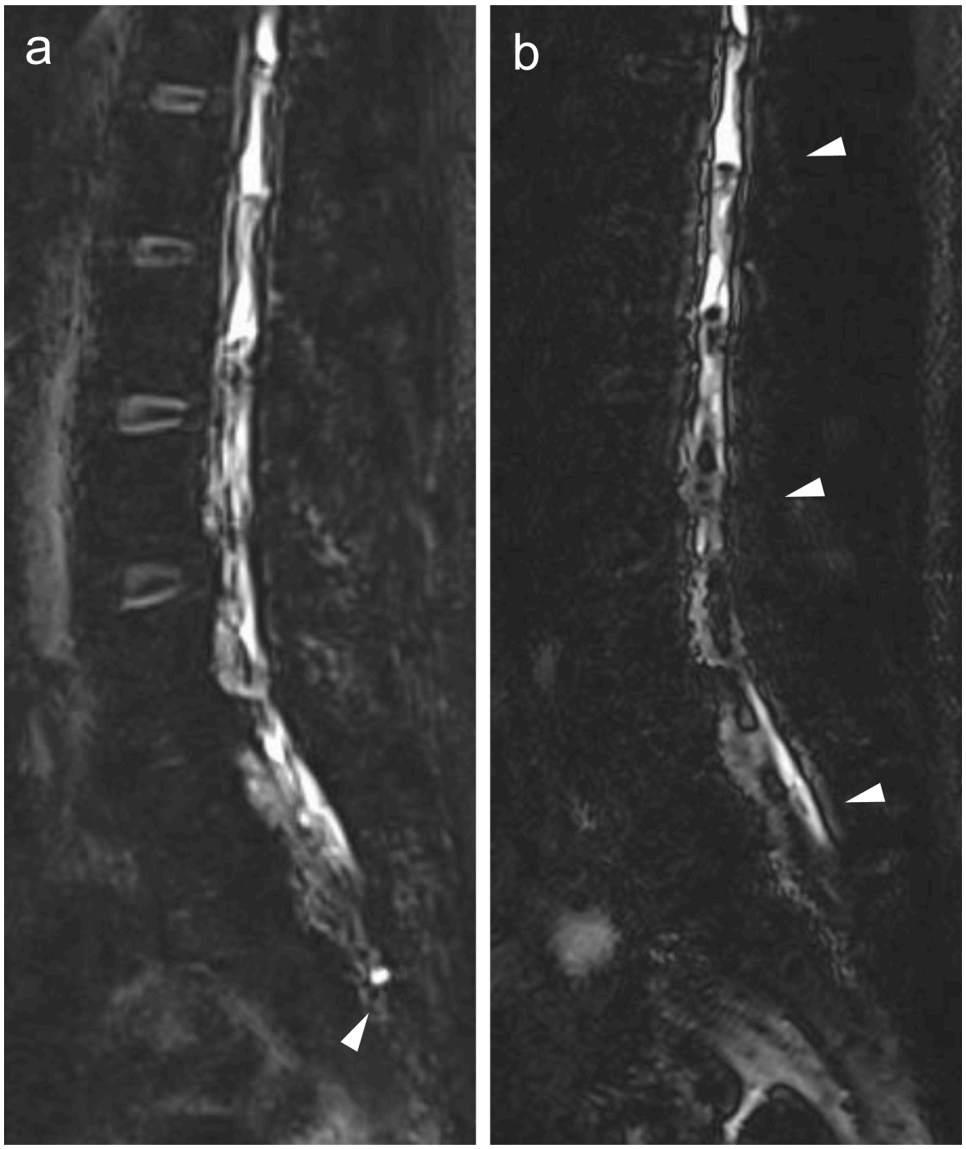


**Fig. 6.** A 40-year-old female with SIH (case 6). Sagittal MR myelography (a) shows a meningeal diverticulum at the left S2 (arrowhead), while post-contrast HT2-FLAIR imaging (b) shows no enhancement of the meningeal diverticulum despite enhancing CSF leaks in the epidural space (arrowheads).

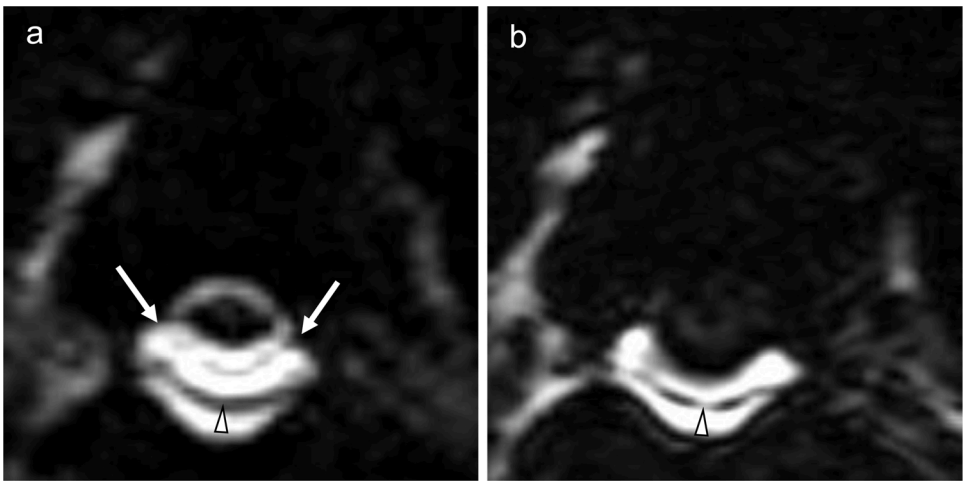


**Fig. 7.** A 31-year-old male with SIH (case 9). Axial MR myelography (a) shows the dilated epidural venous plexus (arrowhead) within epidural fluid collection and the dura mater (arrows). Post-contrast HT2-FLAIR imaging (b) shows no enhancement of the epidural venous plexus (arrowhead) with the enhanced CSF leak. Furthermore, CSF is not enhanced in the subarachnoid space.

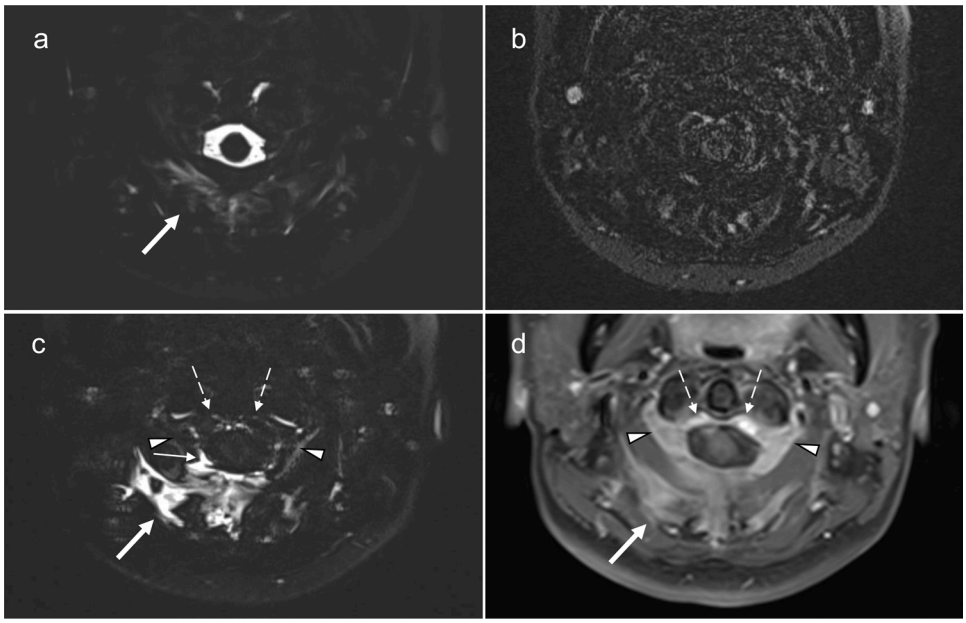


**Fig. 8.** A 50-year-old female with SIH (case 4, same patient as in Fig. 3). Axial MR cisternography (a) of the head shows the C1-2 sign (arrow). In contrast to pre-contrast HT2-FLAIR imaging (b), post-contrast HT2-FLAIR imaging (c) shows contrast enhancement of the C1-2 sign (arrow), while fat-suppressed T1W imaging (d) shows the weak enhancement of this sign (arrow). This retrospinal fluid collection is continuous with epidural fluid collection (c, small arrow). Of note, the suboccipital cavernous sinus (arrowheads) and epidural venous plexus (dotted arrows) show no or weaker contrast enhancement on post-contrast HT2-FLAIR imaging (c) than on T1W imaging (d). These venous structures exhibit stronger contrast enhancement than CSF leaks on T1W imaging.

with greater contrast between T1 shortening material and background tissues.

To the best of our knowledge, this is the first study to demonstrate the contrast enhancement of CSF leaks using HT2-FLAIR imaging. Previous studies may not have reported this phenomenon because T1W imaging cannot identify contrast material in CSF leaks due to its low concentrations. On the other hand, post-contrast T1W imaging may enhance vessel signals due to high concentrations of gadolinium, while HT2-FLAIR imaging may suppress vessel signals and increase contrast between vessels and CSF leaks, which facilitates the differentiation of CSF leaks from vessels (Fig. 7). The present study revealed contrast enhancement of the suboccipital cavernous sinus and epidural venous plexus on post-contrast T1W spin echo images (Fig. 8), which may be explained by the loss of flow voids in spin echo techniques due to slow flow in these vessels. Additionally, the contrast enhancement of these venous structures was stronger than that of CSF leaks on T1W images, reflecting higher concentrations of gadolinium within the veins. On the other hand, HT2-FLAIR imaging showed no or only the weak enhancement of these venous structures, while CSF leaks were strongly enhanced. The difference in contrast enhancement between veins and CSF leaks was also observed on spinal HT2-FLAIR images (Figs. 4 and 5). A previous study demonstrated that 3D FLAIR imaging was more sensitive to not only slow flow, but also lower concentrations of gadolinium than T1W imaging [29]. Therefore, HT2-FLAIR imaging has the capacity to suppress signals from slow-flow vessels with high intravascular concentrations of gadolinium. Although it was not possible to completely rule out the presence of veins in some contrast-enhanced structures on HT2-FLAIR images, contrast enhancement was considered to predominantly occur in CSF leaks, not veins.

Epidural fluid collection represents fluid signal intensity outside the dura mater within the spinal canal. Epidural fluid collection generally does not localize the precise site of a leak and frequently extends along multiple spinal levels. Nevertheless, this is a sensitive feature for diagnosing the presence of CSF leaks, particularly when T2W imaging is used to evaluate suspected SIH. Regarding the identification of epidural fluid collection, the present study showed that HT2-FLAIR imaging was superior to MR myelography (Figs. 2 and 4).

The three critical factors that influence the identification of epidural

fluid collection are: 1) detection of the dura mater, 2) a sufficient volume of CSF leakage for diagnosis, and 3) the differentiation of epidural fat from a CSF leak. Regarding the first factor, since CSF is enhanced on HT2-FLAIR images in the epidural space, but not in the arachnoid space, CSF may be identified without the need to consider the dura mater. In the second factor, a previous study demonstrated the diagnostic utility of subtle arched hyperintensity of the interspinous epidural space on sagittal fat-suppressed T2W images in patients with CSF leaks, which was termed the "Dinosaur tail sign" based on its shape [30]. This may reflect a subtle amount of epidural fluid collection and compensatory dilatation of the epidural venous plexus. In the present study, HT2-FLAIR imaging showed this sign more clearly than MR myelography (Fig. 4), and, thus, has the potential to visualize small CSF leaks by increased contrast between CSF leaks and the surrounding structures. Regarding the third factor, in contrast to MR myelography, HT2-FLAIR imaging allows the fat signal to be eliminated by subtracting pre-contrast images from corresponding post-contrast images.

Paraspinal fluid collection is defined as a fluid signal outside of the spine, including CSF leaks around the nerve root sleeve. Previous studies suggested that CSF leaks around the nerve root sleeve indicated the exact CSF leak site [8], while a recent study demonstrated that periradicular leaks were not restricted to the level of the dural defect in patients with CSF leaks after lumbar puncture [15]. Periradicular leaks may not necessarily represent the precise site of a CSF leak and lumbar puncture may cause an iatrogenic CSF leak. Therefore, periradicular leaks need to be cautiously interpreted, particularly when evaluated using imaging modalities with lumbar puncture. Intravenous gadolinium-enhanced MR imaging proposed herein may be more suitable for evaluating periradicular leaks when planning to inject a tracer of CSF, such as a contrast agent or radioactive isotope.

Regarding paraspinal fluid collection, the present study showed that HT2-FLAIR imaging provided the better visualization of leaks than MR myelography (Figs. 2 and 3), which may be attributed to improved contrast between CSF leaks and the surrounding tissues. Previous studies defined the grading of CSF leaks using coronal [16] or axial [10] MR myelography; however, an overlap was reported in MR findings between SIH patients and controls [10]. This may have been due to the hyperintensity of nearby structures, such as fat or blood vessels. In contrast, HT2-FLAIR imaging may identify enhanced CSF leaks, similar to CT myelography and intrathecal gadolinium-enhanced MR myelography, and provide the better visualization of CSF leaks than non-contrast MRI, even when interpreted by radiologists unfamiliar with SIH. Another important reason for the better visualization of leaks on HT2-FLAIR images may be the lack of misinterpretation between meningeal diverticula and CSF leaks (Fig. 6). Meningeal diverticula may occasionally mimic CSF leaks along the nerve root sleeves [8]. Enhanced CSF leaks may be distinguished from meningeal diverticula on HT2-FLAIR images because CSF in the subarachnoid space within meningeal diverticula has no contrast enhancement.

The C1−2 sign is characterized by retrospinal fluid collection at C1−2 in patients with SIH [26]. This sign does not necessarily represent the precise site of a CSF leak and needs to be interpreted with caution. The present study showed the better visualization of this CSF leak with HT2-FLAIR imaging than with MR myelography (Fig. 3). This may be due to the clear differentiation between CSF leaks and unsuppressed fat. Magnetic field inhomogeneity in the neck is caused by anatomical geometry and susceptibility effects, resulting in incomplete fat suppression [31,32]. Although a chemical shift selective (CHESS) prepulse is mainly used for fat suppression, its main limitation is sensitivity to magnetic field homogeneity. Unsuppressed fat tissue may prevent the identification of pathology and mimic CSF leaks. The better visualization of CSF leaks on HT2-FLAIR images may be explained as follows: the canceling of the fat signal by subtraction from pre-contrast images and the enhancement of CSF leaks.

The present study demonstrated that CSF leaks were enhanced on HT2-FLAIR images; however, the underlying mechanisms remain unclear. One potential reason may be the small amount of blood released from torn dura mater vessels. Recent studies reported that SIH was associated with superficial siderosis [33,34]. Superficial siderosis of the central nervous system is characterized by hemosiderin deposition in the subpial layers of the brain and spinal cord. Wilson et al. classified this entity into 2 groups: type 1 (classical) and type 2 (secondary) [34]. Dural abnormality was a potential cause in 83 % of patients with type 1, including ventral thoracic extra-arachnoid CSF collection and nerve root pseudomeningocele. Type 1 superficial siderosis may be a consequence of persistent or recurrent bleeding into the subarachnoid space, possibly from the micro- or venous vasculature at the dural defect. These constellations are supported by increases in red blood cells or xanthochromia within the CSF of patients with SIH [35,36].

We herein demonstrated that CSF was enhanced in the extra-arachnoid space, but not in the subarachnoid space. Although the underlying mechanisms remain unknown, one possible reason is associated with characteristic CSF flow in patients with SIH. Since CSF mainly flows from the subarachnoid space into the extra-arachnoid space through tears at the dura mater, a contrast agent may preferentially accumulate in the extra-arachnoid space. Furthermore, the volume and flow of CSF in the subarachnoid space may contribute to this phenomenon. Since the volume of the subarachnoid space is larger than that of the extra-arachnoid space, extravasated contrast medium may be further diluted within the subarachnoid space. CSF flow within the subarachnoid space may be sufficiently fast to result in a flow-related signal loss effect on 3D FLAIR images [29]. These 2 effects may lead to the preferential enhancement of CSF in the extra-arachnoid space.

The present study had several limitations. It was limited by its retrospective nature and small sample size. Despite small patient cohorts, significant differences were observed in the overall visualization of CSF leaks between the 2 sequences because HT2-FLAIR provided greater sensitivity for CSF leak detection. Furthermore, the use of gadolinium-based contrast material is restricted for patients with renal failure or contrast allergy. In addition, due to incomplete fat suppression, HT2-FLAIR imaging occasionally required the corresponding pre-contrast images to cancel the fat signal in post-contrast images. Further research is warranted to achieve more homogenous and robust fat suppression. Although HT2-FLAIR imaging has the capacity to suppress vessel signals and enhance contrast between veins and CSF leaks, another limitation is that some contrast-enhancing structures may include veins or the dura mater. Other sequences, such as post-contrast T1W imaging, may help to differentiate CSF leaks from these structures. Moreover, HT2-FLAIR imaging offers less anatomical information than fat-suppressed T2W imaging due to the suppression of the background signal, except for contrast material. This disadvantage may decrease the detectability of the 2 main features: other spinal MR findings (a dilated epidural vein or displacement of the dura mater) and structural abnormalities associated with possible causes of SIH (meningeal diverticula, dural tear, or osteophyte).

## 5. Conclusion

In conclusion, the visualization of CSF leaks in patients with SIH was superior with intravenous gadolinium-enhanced HT2-FLAIR imaging than with MR myelography. This method can be useful for identifying spinal CSF leaks.

## Funding

This research was supported by the Japan Agency for Medical Research and Development (AMED) under Grant Number JP20dk0310099.

## Ethical statement

All procedures performed in studies involving human participants

were in accordance with the ethical standards of the institutional and/or national research committee and with the 1964 Helsinki declaration and its later amendments or comparable ethical standards.

## Informed consent

This retrospective study was conducted at a single institution and approved by the Institutional Review Board of our institution. We obtained written informed consent for the procedures and opt-out consent for the use of retrospective clinical data from all patients/ from parents or legal guardian of patient less than 18 years.

## CRediT authorship contribution statement

**Iichiro Osawa:** Conceptualization, Data curation, Formal analysis, Writing - original draft. **Eito Kozawa:** Formal analysis, Methodology, Supervision, Writing - review & editing. **Takashi Mitsufuji:** Data curation, Writing - review & editing. **Toshimasa Yamamoto:** Supervision, Writing - review & editing. **Nobuo Araki:** Funding acquisition, Supervision, Writing - review & editing. **Kaiji Inoue:** Supervision, Writing - review & editing. **Mamoru Niitsu:** Supervision, Writing - review & editing.

## Declaration of Competing Interest

The authors report no declarations of interest.

## Acknowledgments

We thank Mr. Hiroshi Imai of Siemens Healthcare for his technical assistance with this study. We also express our appreciation to all the technicians, nurses, and patients involved with the study.

## References

[1] P.G. Kranz, P.H. Luetmer, F.E. Diehn, T.J. Amrhein, T.P. Tanpitukpongse, L. Gray, Myelographic techniques for the detection of spinal CSF leaks in spontaneous intracranial hypotension, AJR Am. J. Roentgenol. 206 (1) (2016) 8–19.
[2] P.G. Kranz, L. Gray, T.J. Amrhein, Spontaneous intracranial hypotension: 10 myths and misperceptions, Headache 58 (7) (2018) 948–959.
[3] W.I. Schievink, Misdiagnosis of spontaneous intracranial hypotension, Arch. Neurol. 60 (12) (2003) 1713–1718.
[4] B. Mokri, D.G. Piepgras, G.M. Miller, Syndrome of orthostatic headaches and diffuse pachymeningeal gadolinium enhancement, Mayo Clin. Proc. 72 (5) (1997) 400–413.
[5] P.G. Kranz, T.P. Tanpitukpongse, K.R. Choudhury, T.J. Amrhein, L. Gray, Imaging signs in spontaneous intracranial hypotension: prevalence and relationship to CSF pressure, AJNR Am. J. Neuroradiol. 37 (7) (2016) 1374–1378.
[6] J.L. Chazen, J.F. Talbott, J.E. Lantos, W.P. Dillon, MR myelography for identification of spinal CSF leak in spontaneous intracranial hypotension, AJNR Am. J. Neuroradiol. 35 (10) (2014) 2007–2012.
[7] J.M. Hoxworth, T.L. Trentman, A.L. Kotsenas, K.R. Thielen, K.D. Nelson, D. W. Dodick, The role of digital subtraction myelography in the diagnosis and localization of spontaneous spinal CSF leaks, AJR Am. J. Roentgenol. 199 (3) (2012) 649–653.
[8] A. Watanabe, T. Horikoshi, M. Uchida, H. Koizumi, T. Yagishita, H. Kinouchi, Diagnostic value of spinal MR imaging in spontaneous intracranial hypotension syndrome, AJNR Am. J. Neuroradiol. 30 (1) (2009) 147–151.
[9] P.H. Tsai, J.L. Fuh, J.F. Lirng, S.J. Wang, Heavily T2-weighted MR myelography in patients with spontaneous intracranial hypotension: a case-control study, Cephalalgia 27 (8) (2007) 929–934.
[10] C.H. Chen, J.H. Chen, H.C. Chen, J.W. Chai, P.L. Chen, C.C. Chen, Patterns of cerebrospinal fluid (CSF) distribution in patients with spontaneous intracranial hypotension: assessed with magnetic resonance myelography, J. Chin. Med. Assoc. 80 (2) (2017) 109–116.
[11] S. Albayram, F. Kilic, H. Ozer, S. Baghaki, N. Kocer, C. Islak, Gadolinium-enhanced MR cisternography to evaluate dural leaks in intracranial hypotension syndrome, AJNR Am. J. Neuroradiol. 29 (1) (2008) 116–121.
[12] B. Mokri, Radioisotope cisternography in spontaneous CSF leaks: interpretations and misinterpretations, Headache 54 (8) (2014) 1358–1368.
[13] E. Hattingen, R. DuMesnil, U. Pilatus, A. Raabe, T. Kahles, J. Beck, Contrast-enhanced MR myelography in spontaneous intracranial hypotension: description of an artefact imitating CSF leakage, Eur. Radiol. 19 (7) (2009) 1799–1808.
[14] K. Sakurai, M. Nishio, S. Sasaki, H. Ogino, J. Tohyama, K. Yamada, Y. Shibamoto, Postpuncture CSF leakage: a potential pitfall of radionuclide cisternography, Neurology 75 (19) (2010) 1730–1734.
[15] Y.F. Wang, J.L. Fuh, J.F. Lirng, S.P. Chen, S.S. Hseu, J.C. Wu, S.J. Wang, Cerebrospinal fluid leakage and headache after lumbar puncture: a prospective non-invasive imaging study, Brain 138 (Pt 6) (2015) 1492–1498.
[16] H.M. Yoo, S.J. Kim, C.G. Choi, D.H. Lee, J.H. Lee, D.C. Suh, J.W. Choi, K.S. Jeong, S.J. Chung, J.S. Kim, S.C. Yun, Detection of CSF leak in spinal CSF leak syndrome using MR myelography: correlation with radioisotope cisternography, AJNR Am. J. Neuroradiol. 29 (4) (2008) 649–654.
[17] Y.F. Wang, J.F. Lirng, J.L. Fuh, S.S. Hseu, S.J. Wang, Heavily T2-weighted MR myelography vs CT myelography in spontaneous intracranial hypotension, Neurology 73 (22) (2009) 1892–1898.
[18] Y. Tomoda, Y. Korogi, T. Aoki, T. Morioka, H. Takahashi, M. Ohno, I. Takeshita, Detection of cerebrospinal fluid leakage: initial experience with three-dimensional fast spin-echo magnetic resonance myelography, Acta radiol. 49 (2) (2008) 197–203.
[19] E.C. Williams, B.R. Buchbinder, S. Ahmed, T.A. Alston, J.P. Rathmell, J. Wang, Spontaneous intracranial hypotension: presentation, diagnosis, and treatment, Anesthesiology 121 (6) (2014) 1327–1333.
[20] S. Naganawa, The technical and clinical features of 3D-FLAIR in neuroimaging, Magn. Reson. Med. Sci. 14 (2) (2015) 93–106.
[21] S. Naganawa, M. Yamazaki, H. Kawai, K. Bokura, M. Sone, T. Nakashima, Visualization of endolymphatic hydrops in Meniere's disease with single-dose intravenous gadolinium-based contrast media using heavily T(2)-weighted 3D-FLAIR, Magn. Reson. Med. Sci. 9 (4) (2010) 237–242.
[22] S. Naganawa, M. Yamazaki, H. Kawai, M. Sone, T. Nakashima, Contrast enhancement of the anterior eye segment and subarachnoid space: detection in the normal state by heavily T2-weighted 3D FLAIR, Magn. Reson. Med. Sci. 10 (3) (2011) 193–199.
[23] W.I. Schievink, D.W. Dodick, B. Mokri, S. Silberstein, M.G. Bousser, P.J. Goadsby, Diagnostic criteria for headache due to spontaneous intracranial hypotension: a perspective, Headache 51 (9) (2011) 1442–1444.
[24] Headache Classification Committee of the International Headache Society (IHS), The international classification of headache disorders, 3rd edition, Cephalalgia 38 (1) (2018) 1–211.
[25] T. Yagi, T. Horikoshi, N. Senbokuya, H. Murayama, H. Kinouchi, Distribution patterns of spinal epidural fluid in patients with spontaneous intracranial hypotension syndrome, Neurol. Med. Chir. (Tokyo) 58 (5) (2018) 212–218.
[26] W.I. Schievink, M.M. Maya, J. Tourje, False localizing sign of C1-2 cerebrospinal fluid leak in spontaneous intracranial hypotension, J. Neurosurg. 100 (4) (2004) 639–644.
[27] M. Nagayama, Y. Watanabe, A. Okumura, Y. Amoh, S. Nakashita, Y. Dodo, High-resolution single-slice MR myelography, AJR Am. J. Roentgenol. 179 (2) (2002) 515–521.
[28] S. Naganawa, T. Koshikawa, T. Nakamura, H. Kawai, H. Fukatsu, T. Ishigaki, T. Komada, K. Maruyama, O. Takizawa, Comparison of flow artifacts between 2D-FLAIR and 3D-FLAIR sequences at 3 T, Eur. Radiol. 14 (10) (2004) 1901–1908.
[29] H. Fukuoka, T. Hirai, T. Okuda, Y. Shigematsu, A. Sasao, E. Kimura, T. Hirano, S. Yano, R. Murakami, Y. Yamashita, Comparison of the added value of contrast-enhanced 3D fluid-attenuated inversion recovery and magnetization-prepared rapid acquisition of gradient echo sequences in relation to conventional postcontrast T1-weighted images for the evaluation of leptomeningeal diseases at 3T, AJNR Am. J. Neuroradiol. 31 (5) (2010) 868–873.
[30] K. Sakurai, M. Kanoto, M. Nakagawa, M. Shimohira, A.M. Tokumaru, M. Kameyama, K. Shimoji, S. Morimoto, N. Matsukawa, M. Nishio, Y. Shibamoto, Dinosaur tail sign: a useful spinal MRI finding indicative of cerebrospinal fluid leakage, Headache 57 (6) (2017) 917–925.
[31] J.J. Akbar, P.H. Luetmer, K.M. Schwartz, C.H. Hunt, F.E. Diehn, L.J. Eckel, The role of MR myelography with intrathecal gadolinium in localization of spinal CSF leaks in patients with spontaneous intracranial hypotension, AJNR Am. J. Neuroradiol. 33 (3) (2012) 535–540.
[32] Z. Metafratzi, M.I. Argyropoulou, C. Mokou-Kanta, S. Konitsiotis, A. Zikou, S. C. Efremidis, Spontaneous intracranial hypotension: morphological findings and CSF flow dynamics studied by MRI, Eur. Radiol. 14 (6) (2004) 1013–1016.
[33] N. Kumar, Neuroimaging in superficial siderosis: an in-depth look, AJNR Am. J. Neuroradiol. 31 (1) (2010) 5–14.
[34] D. Wilson, F. Chatterjee, S.F. Farmer, P. Rudge, M.O. McCarron, P. Cowley, D. J. Werring, Infratentorial superficial siderosis: classification, diagnostic criteria, and rational investigation pathway, Ann. Neurol. 81 (3) (2017) 333–343.
[35] B. Mokri, Spontaneous low pressure, low CSF volume headaches: spontaneous CSF leaks, Headache 53 (7) (2013) 1034–1053.
[36] D. Holle, I.E. Sandalcioglu, E.R. Gizewski, S. Asgari, D. Timmann, H.C. Diener, C. Weimar, Association of superficial siderosis of the central nervous system and low pressure headache, J. Neurol. 255 (7) (2008) 1081–1082.